

Chapter 12

Supercritical Fluid Technology as a Tool to Prepare Gradient Multifunctional Architectures Towards Regeneration of Osteochondral Injuries



Ana Rita C. Duarte, Vitor E. Santo, Manuela E. Gomes, and Rui L. Reis

Abstract Platelet lysates (PLs) are a natural source of growth factors (GFs) known for its stimulatory role on stem cells which can be obtained after activation of platelets from blood plasma. The possibility to use PLs as growth factor source for tissue healing and regeneration has been pursued following different strategies. Platelet lysates are an enriched pool of growth factors which can be used as either a GFs source or as a three-dimensional (3D) hydrogel. However, most of current PLs-based hydrogels lack stability, exhibiting significant shrinking behavior. This chapter focuses on the application of supercritical fluid technology to develop three-dimensional architectures of PL constructs, crosslinked with genipin. The proposed technology allows in a single step operation the development of mechanically stable porous structures, through chemical crosslinking of the growth factors present in the PL pool, followed by supercritical drying of the samples. Furthermore gradient structures of PL-based structures with bioactive glass are also presented and are described as an interesting approach to the treatment of osteochondral defects.

Keywords Supercritical fluid technology · Platelet lysate · Genipin · Polymerization · Gradient structures

A. R. C. Duarte (✉) · V. E. Santo · M. E. Gomes · R. L. Reis
3B's Research Group—Biomaterials, Biodegradables and Biomimetics, European Institute of Excellence on Tissue Engineering and Regenerative Medicine, University of Minho, Barco/Guimarães, Portugal

ICVS/3B's—PT Government Associate Laboratory, Braga/Guimarães, Portugal
e-mail: aduarte@dep.uminho.pt

© Springer International Publishing AG, part of Springer Nature 2018
J. M. Oliveira et al. (eds.), *Osteochondral Tissue Engineering*,
Advances in Experimental Medicine and Biology 1058,
https://doi.org/10.1007/978-3-319-76711-6_12

265

12.1 Introduction

Full thickness chondral and osteochondral defects and early osteoarthritis represent one of the most significant challenges facing the global health care community due to the limited healing potential of articular cartilage, resulting in chronic degeneration. Osteochondral tissue is a gradual transition from cartilage to bone in which the key constituents of each tissue undergo an exchange in predominance. Structurally, the osteochondral interface is the connection between a layer of hyaline cartilage and underlying bone and it is crucial for load transfer between bone and cartilage [1, 2]. The most commonly used standard therapies for treating articular cartilage defects are generally successful for pain relief and improved function but do not restore the articular cartilage and subchondral bone completely, leading to degeneration over time [3]. Tissue Engineering (TE) offers an alternative approach to the current treatments, aiming at the regeneration of tissues through the use of cells within a supporting matrix that may also incorporate biomolecules (e.g., growth factors—GFs) that enhance cell function and/or tissue regeneration [4].

The concept of osteochondral TE, a hybrid of bone and cartilage regeneration, has attracted considerable attention, particularly as a technique for promoting superior cartilage integration and as a treatment for osteochondral defects [5]. The engineering of complex tissues, which involve multiple cell types organized in specific patterns, such as the orthopedic interface [6], is still a rather challenging task and it is recognized that the effective regeneration of these tissues has not been fully attained. For osteochondral scaffolds, additional design criteria should be considered to achieve the best possible simultaneous growth of the two independent tissues involved. A single scaffold with a homogeneous structure may not be the ideal support for such applications and therefore a bilayered scaffold combining parts with differing physical and chemical properties might be the most suitable approach to promote the simultaneous individual growth of cartilage and bone on a single integrated implant. This may require the use of biphasic constructs with areas with distinct mechanical, structural, and molecular properties [7, 8]. Some studies have focused on the development of two layers with different architecture and mechanical properties [9, 10], whereas others have focused more on the delivery of bioactive agents distributed in the structure with a concentration gradient [8], to promote the formation of a calcified matrix on the bone side of the interface and a cartilage-type extracellular matrix (ECM) on the opposite side of the interface. Natural and synthetic polymers have been used to produce these scaffolds but another interesting material that can be used to create new cell-laden structures comprises the use of Platelet Lysate (PL). In the past three decades, the increasing knowledge on the physiological roles of platelets in wound healing and tissue injury suggests the potential of using platelets as therapeutic tools [11]. Platelets are anucleate cytoplasmic fragments which form an intracellular storage pool of proteins vital to wound healing. Upon activation of platelets, lysis and subsequent release of several GFs occurs, naturally constituting a pool of bioactive factors at physiological concentrations. This protein concentrate is known to play key roles in tissue healing and

stimulation of cell expansion and recruitment. Simultaneously, it can also form a tridimensional network amenable to act as support for cell culture. Previous research studies have reported the development of PL-based scaffolds/hydrogels; however, they typically show high levels of shrinkage and lack long-term stability, requiring combination with other materials to acquire mechanical integrity [12].

In this chapter, we explore a new TE approach targeting the treatment of osteochondral defects. The strategy proposed consists in the combination of a novel autologous PL-based gradient scaffold to promote the regeneration of the orthopedic interface using supercritical fluid technology. Our aim was the development of a PL-based gradient scaffold crosslinked with genipin. The bulk component is based on the genipin-crosslinked PL network produced by supercritical fluid-assisted process. One of the sides of the scaffold (the one that faces the bone layer) is enriched with calcium phosphates (CaP) or Bioglass[®] to enhance osteoinductivity and mechanical properties. The other side (facing cartilage) is void of ceramic component. Although the use of PL in tissue regeneration strategies is not new, this project presents the novelty of simultaneously using this blood derivative as gradient-inducing scaffolding system for the osteochondral defect, and simultaneously as a source of bioactive proteins to promote the regeneration of the tissues.

Supercritical fluid technology has already proven to be feasible for many pharmaceutical applications and it has also been demonstrated to be a valid alternative to conventional processes for the preparation of tridimensional scaffolds due to its mild processing parameters [13–16].

12.2 Supercritical Fluid Technology

The development of 3D architectures for TE and regenerative medicine using supercritical fluid technology can take advantage of different properties of a supercritical fluid and several techniques have already been reported. The development of matrices for the regeneration of osteochondral defects explored in this chapter relies on the principles of the supercritical assisted phase inversion. In this method, two mechanisms occur at the same time: (1) the diffusion of the supercritical fluid into the protein solution, which results on the precipitation of the proteins from the aqueous solution; and (2) the removal of the solvent by the supercritical fluid. The phase separation and precipitation of the proteins to form a porous scaffold is favored by a high solubility between the solvent and the anti-solvent, i.e., a higher affinity of the solvent to the carbon dioxide [17]. The mutual affinity of water and carbon dioxide is very low due to their opposite polarity. To improve polarity of carbon dioxide, a small amount of an entrainer or cosolvent can be mixed with the gas. This can, in some cases, produce dramatic effects on the solvent power, greatly enhancing the solubility and/or affinity between two components [18]. Accordingly, it has been described in the literature, the successful preparation of chitosan membranes from dilute acetic acid aqueous solutions by supercritical assisted phase inversion [19]. On another hand, organic solvents have been reported to promote protein

precipitation, at moderate concentration, without affecting the functional properties of the proteins. Ethanol is a particularly interesting solvent and previous studies have demonstrated that processing proteins in the presence of small amounts of ethanol does not compromise protein activity. In particular, we have reported the development of 3D architectures of PDLLA scaffolds with PL-loaded nanoparticles, in the presence of small amounts of ethanol. The results obtained suggest that the activity of the GFs was not compromised and the ability to guide stem cell differentiation was maintained [13, 16].

12.3 Development of PL-Based 3D Multifunctional Architectures

Osteochondral TE has shown an increasing development and investment towards the design of suitable strategies to stimulate the regeneration of damaged cartilage and underlying subchondral bone tissue [20–23]. The use of two scaffolds with specific properties for bone and cartilage architectures, combined at the time of implantation as a multilayered structure was one of the first approaches for regeneration of large osteochondral defects. New design approaches have been proposed, including the use of bilayered scaffolds with distinct properties in each side of the construct, and the use of continuous gradient scaffolds. Different gradient structures have been proposed, focusing either on ranges of morphological features, mechanical properties, presentation of bioactive molecules, or combinations of these [8–10, 24, 25].

Most of these structures have been designed using natural and/or synthetic polymers. Due to its bioactivity and structural potential, PL also arises as potential bulk material for the generation of novel scaffolds for osteochondral regeneration. The pool of GFs present in PL comprises several of the signalling molecules known to induce cell expansion and migration. Moreover, some of them are also known to stimulate osteogenic and chondrogenic differentiation of human stem cells [13, 26]. Moreover, PL can be obtained from the patient's own blood, allowing us to pursue an autologous approach and eliminating immunogenic and disease transmission concerns [11]. Most of the strategies involving PL for the generation of 3D constructs either use polymeric networks absorbed and functionalized with PL [27, 28] or calcium-activated PL hydrogels for cell encapsulation. Hydrogels using PL as bulk material typically show fast degradation and relative instability, thus limiting their application potential [12]. Moreover, their mechanical properties are also poor and tend to be suitable for regeneration of soft tissues [11]. The osteochondral region of joints is a particularly mechanically demanding microenvironment and requires the application of biomaterials capable of withstanding an array of physical stimuli [1, 29–31]. To our knowledge, there is not published data regarding the use of PL as bulk material for the development of advanced scaffolds for osteochondral regeneration.

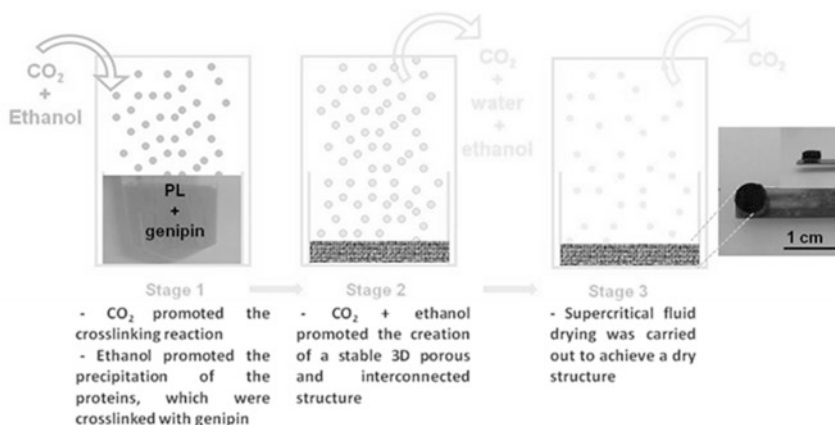


Fig. 12.1 Schematic representation of the supercritical fluid technique designed for the preparation of PL-based 3D architectures

The technique herein reported leads to the generation of a gradient scaffold, produced in a single step procedure, in which the simultaneous precipitation of PL proteins and the establishment of crosslinking bridges between the amino groups of the proteins and genipin takes place. Figure 12.1 presents a summary of the process.

One of the advantages of the use of supercritical fluid technology is the fact that single unit operations can be designed, avoiding the need for several subsequent steps of production. As a result, a 3D porous scaffold is obtained. Briefly, PL mixed with the crosslinker agent (genipin) is placed inside a high-pressure vessel, heated to the desired temperature (35–40 °C), and pressurized with carbon dioxide until the set pressure of the experiment (80–140 bar). The crosslinking reaction is allowed to take place for a pre-determined period of time and afterwards a stream of ethanol + CO₂ passes through the vessel in order to promote phase inversion and extract the aqueous solution. Finally, the high-pressure chamber is flushed by adding fresh CO₂ under the same conditions in order to extract the residual ethanol and the system is slowly depressurized.

Genipin is a naturally occurring crosslinking agent which was chosen, particularly due to its low cytotoxicity and to the ability to bind proteins or amino-acids between adjacent amino groups, forming blue pigments [32]. PL, on the other hand, is a protein concentrate, thus offering a high number of crosslinking sites to interact with the ester groups of genipin, leading to the formation of secondary amide linkages. The identification of specific proteins involved in the crosslinking reaction is not straightforward due to the enriched composition of PL. It has been reported that the mechanisms of crosslinking reactions with genipin are different at different pH values [33–35]. Among the studies documented, it has been suggested that the acid catalysis is necessary for the crosslinking reaction to occur. The advantages of the crosslinking reaction under dense carbon dioxide atmosphere are related with the acidification of aqueous solutions after the solubilization of CO₂ molecules, which,

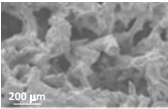
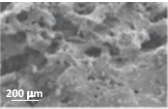
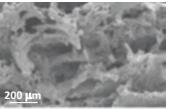
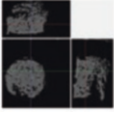
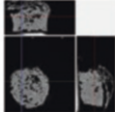
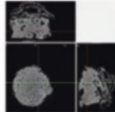
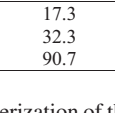
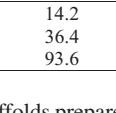
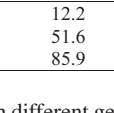
Sample	PL _{LXL}	PL _{MXL}	PL _{HXL}
SEM			
Micro-CT			
2D sections			
Porosity (%)	17.3	14.2	12.2
Interconnectivity (%)	32.3	36.4	51.6
Mean pore size (μm)	90.7	93.6	85.9

Fig. 12.2 Morphological characterization of the scaffolds prepared with different genipin concentrations: SEM and micro-CT 2D micrographs of cross sections of the PL scaffolds

depending on the operating conditions, can reach pH values up to 3. Previous work reported in the literature has shown though that the activity of the proteins is not compromised by the low pH at which the process takes place [36]. In fact, we have previously developed genipin-crosslinked PL membranes for cell culture applications, with reduced toxicity [37].

The production of PL scaffolds was pursued by using three different genipin concentrations. Genipin was dissolved in PL suspensions at final concentration range of 0.18–0.25% (w/v) before initiation of the supercritical fluid process. The optimal reaction time was evaluated and it was found to be 1 h. Three conditions were defined according to their classification of crosslinking degree: low (PL_{LXL}), medium (PL_{MXL}), and high crosslinking degree (PL_{HXL}). Morphological analysis of the three categories of architectures was performed by Scanning Electron Microscopy (SEM) and micro-Computed Tomography (micro-CT). Qualitative and quantitative outputs extracted from these characterization methods are shown in Fig. 12.2.

The morphological analysis of the scaffolds provided the first hints on their feasibility to act as structural support for growth and proliferation of seeded cells. The crosslinking degree showed influence on the morphological properties of the 3D structures, as it can be seen from the quantitative measurement of % of porosity, interconnectivity, and mean pore size. Mean pore size ranged between 85.9 and 93.6 μm, typically considered an appropriate dimension for cell migration through the pore. However, the obtained structures were highly compact, with porosity levels ranging from 12.2 to 17.3%, from the highest crosslinked scaffold to the lowest, respectively. This indicates the formation of highly packed architectures, which could be confirmed by SEM micrographs of cross sections of these PL scaffolds. Moreover, interconnectivity levels were also low, curiously being the lowest for the PL_{LXL} condition (32.3%) and the highest for PL_{HXL} (51.6%). These levels of porosity and interconnectivity could discourage further studies; however, we had evidence from previous studies from our laboratory that even PL-enriched structures with

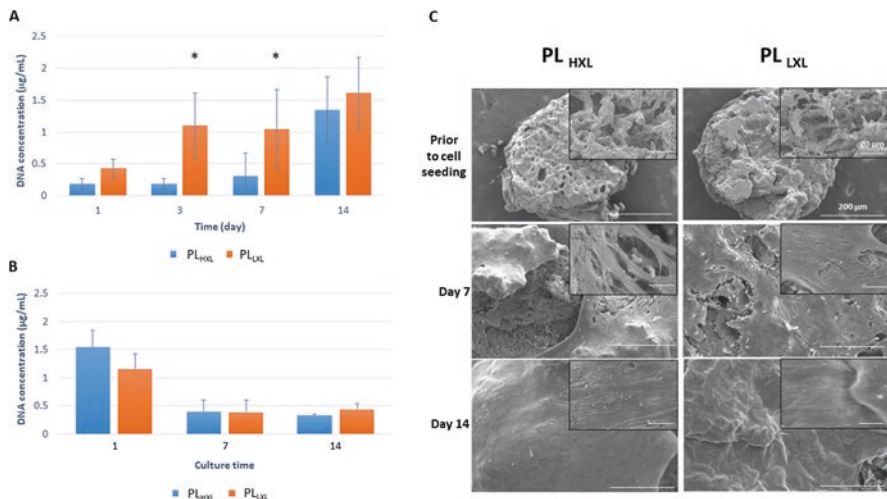


Fig. 12.3 Cell adhesion and proliferation in PL_{LXL} and PL_{HXL} scaffolds. (a) Measurement of DNA concentration of constructs seeded with ATDC5 cells; (b) Measurement of DNA concentration of constructs seeded with hASCs; (c) SEM micrographs of PL_{LXL} and PL_{HXL} scaffolds prior and after seeding with hASCs. * Represents a statistically significant difference ($p < 0.05$) between DNA concentration levels of PL_{LXL} and PL_{HXL} scaffolds

poor initial porosity could act as templates for cell culture. The progressive dissolution of the PL bulk matrix leads to the cumulative formation of pores within the structure, enabling cell migration and colonization of the inner regions of the construct [38]. At the same time, we also expected a delayed dissolution profile due to the covalent reinforcement induced by genipin crosslinking.

PL_{LXL} and PL_{HXL} scaffold formulations were selected to perform the cellular studies. Figure 12.3 depicts the results from the cell seeding of chondrocyte cell line—ATDC5 (Fig. 12.3a) and human adipose-derived stromal cells—hASCs (Fig. 12.3b, c).

The response of cells to the developed PL-based scaffolds was evaluated by overall DNA quantification along culture period and by characterization of cellular morphology and organization during time. Two different cell types were used: one chondrocytic cell line (ATDC5) and human mesenchymal stem cells isolated from adult adipose-derived tissue stromal cells. Figure 12.3a shows a progressive increase of DNA concentration in ATDC5 cultures for both conditions, indicating that PL scaffolds act as templates for cell proliferation. At days 3 and 7 of culture, PL_{LXL} showed significantly higher DNA levels, thus indicating an enhanced cellular proliferation for the lowest crosslinked structures. At day 14, there were no significant differences in cumulative cell number between the scaffolds with distinct degrees of crosslinking.

Figure 12.3b reports DNA concentration of hASCs up to 14 days of culture. For this condition, there were no differences between the highest and the lowest crosslinked structures. At day 1, DNA concentration was the highest for these cultures,

decreasing during the first week and remaining constant up to 14 days of *ex vivo* culture. These cells were cultured with chondrogenic differentiation medium supplemented with the typical factors for stimulation of *in vitro* chondrogenesis, with the exception of Transforming Growth Factor- β (TGF- β), which was available as a component of the PL concentrate. Therefore, the lack of cell expansion throughout the 14 days of culture period was not surprising, as cells were more committed to differentiation processes rather than cell division. Figure 12.3c provides a morphological and qualitative characterization of cell adhesion, proliferation, and colonization of the PL-based constructs. It was possible to observe that hASCs managed to adhere to the surface of the scaffolds, presenting the typical elongated morphology of these cells when adhered onto a substrate. At day 14, a confluent layer of cells was evident for both scaffold formulations, thus confirming that cells were proliferating and that the material was not inducing cytotoxicity to the adhered cells. From these results, both high- and low-crosslinked PL scaffolds were viable templates for cell culture and could be further explored for osteochondral tissue engineering applications.

12.4 Development of Gradient PL-Based Architectures for Osteochondral Tissue Regeneration Applications

The main challenge in developing a functional osteochondral implant is related with the different features required for each region of the defect. While the scaffold region exposed to the cartilage side should possess lower mechanical properties, the component that aims to regenerate the subchondral bone requires strong mechanical properties and mineralization capacity, which may not be achieved solely by the crosslinking of PL with genipin. Bioactivity of the structure can be enhanced by the presence of ceramics presenting inherent osteoinductive properties. In this sense, the preparation of biodegradable composites containing hydroxyapatite-based calcium phosphates (CaP) or Bioglass[®] (BG) is a viable complement to the construct design.

Taking this in consideration, we have selected the condition PL_{HXL} for the generation of gradient scaffolds, due to its superior interconnectivity levels. The incorporation of the inorganic material in the 3D structures only required one additional step to the protocol already described for the preparation of PL scaffolds, and consisted in the dispersion of BG particles within the PL suspension prior to the supercritical fluid processing steps. The incorporation of inorganic material in the 3D structures did not compromise the generation of the structures and led to the natural formation of a bilayered architecture: one BG-enriched region and other BG-poor phase (as presented in Fig. 12.4).

Significant structural changes were observed regarding porosity (53%), interconnectivity (78%), and average pore size (177.9 μm) in the BG-enriched region. The

Fig. 12.4 SEM micrograph of a cross section of the PL_{HXL}-BG scaffold, clearly depicting two distinct regions: one BG-enriched layer on the lower section of the scaffold and one BG-poor region on the upper part of the architecture

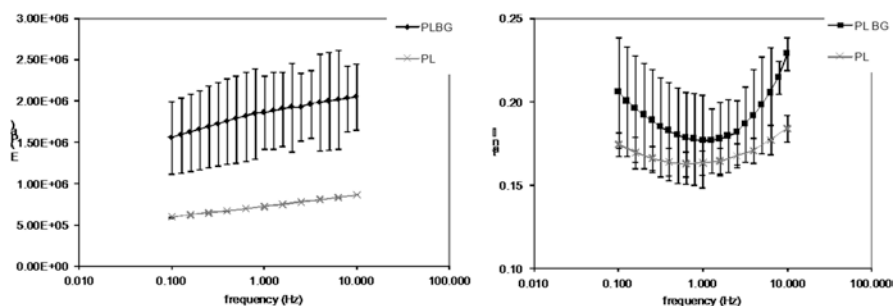
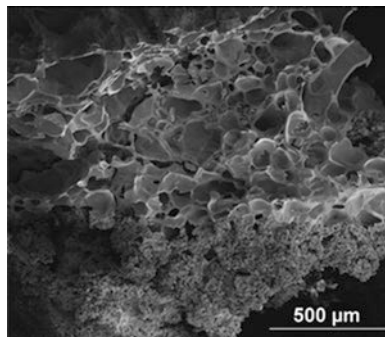


Fig. 12.5 Mechanical properties of the PL_{HXL}-BG and PL_{HXL} scaffolds: Storage modulus (E') curves as function of frequency and loss factor ($\tan \delta$) curves as function of frequency

BG-poor layer also presented significant changes in comparison with the PL_{HXL} scaffolds produced in the absence of BG particles.

The impact of incorporation of BG particles and architectural changes of the scaffold on the overall mechanical performance of the constructs was evaluated by Dynamic Mechanical Analysis (DMA). Mechanical analysis of the scaffolds was performed in dynamic compression mode on hydrated samples using DMA measurements. Figure 12.5 shows the isothermal response of the various samples as a function of frequency in terms of storage modulus (E') and the loss factor ($\tan \delta$).

The presence of BG particles in the 3D scaffold led to improved mechanical properties, particularly on the storage modulus, throughout the range of frequencies of compression forces imposed in the scaffolds. Whereas for PL_{HXL} scaffolds, the elastic modulus was found between 0.55 and 0.8 MPa, the elastic modulus of PL_{HXL}-BG scaffolds was comprised between 1.5 and 2 MPa. This was an expected observation and it has been reported in previous studies as BG particles may also act as reinforcement fillers enhancing the mechanical properties of the 3D structures in which they are dispersed [39, 40].

The following step was focused on the evaluation of the bioactivity of the PL_{HXL} and PL_{HXL}-BG samples, thus validating the influence of BG addition on the deposition of mineralized matrix. To attain this, the scaffolds were immersed in a simulated

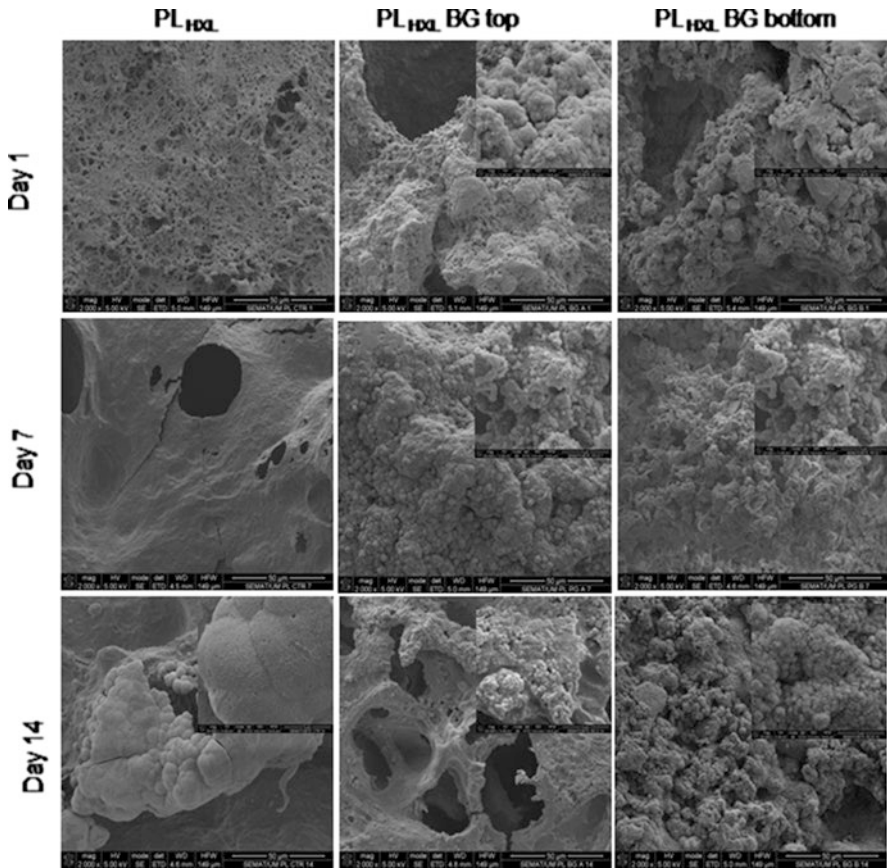


Fig. 12.6 SEM micrographs of PL_{HXL} and PL_{HXL} -BG scaffolds after immersion in SBF solution for 1, 7, and 14 days

body fluid (SBF) solution and the formation of CaP crystals was followed after 1, 7, and 14 days. Figure 12.6 shows the SEM micrographs of the scaffolds after immersion in SBF. The PL_{HXL} -BG were analyzed in the BG-rich zone (bottom) and BG-poor zone (top).

We could observe that the PL_{HXL} scaffolds were bioactive per se, although the presence of BG accelerated the nucleation and growth of an apatite layer. The typical cauliflower-like crystals, characteristic of hydroxyapatite (HA), could be detected in the PL_{HXL} -BG scaffolds after 7 days of immersion in SBF. These findings were checked by infrared spectroscopy, which confirmed the chemical nature of the formed crystals (Fig. 12.7).

The strong FTIR bands characteristic of phosphate and carbonate in hydroxyapatite crystals, namely ν_3 - PO_4 at 1040 cm^{-1} and ν_3 - CO_3 in the region $1400\text{--}1550\text{ cm}^{-1}$, can be observed in the spectra of PL_{HXL} and PL_{HXL} BG, with greater intensity on the PL_{HXL} BG. In the PL scaffolds loaded with BG, it is also possible to identify other

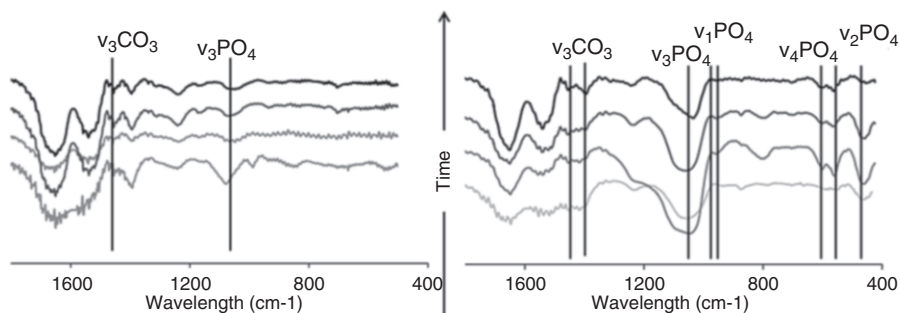


Fig. 12.7 FTIR analysis of the scaffolds immersed in SBF solution. FTIR spectra on the left is representative of the PL_{HXL} scaffold. The spectra on the right is representative of the PL_{HXL}-BG scaffolds

spectral characteristic bands of hydroxyapatite [41], such as ν_1 -PO₄ at 962 cm⁻¹, ν_2 -PO₄ at 472 cm⁻¹, and ν_4 -PO₄ at 575 and 561 cm⁻¹.

The presence of BG particles was shown to be important to tune the rate of formation of the HA layer on the surface of the scaffolds and to be able to synchronize it with the sequence of cellular changes that take place upon new tissue formation.

12.5 Conclusions

The development of mechanically stable 3D architectures based on PL as bulk material with potential application in TE and regenerative medicine was discussed in this chapter. Herein, we report a new methodology based on supercritical fluid technology for the development of a stable PL-based scaffold crosslinked with genipin. PL is interesting source of GFs which can be obtained after activation of platelets from the patient's blood plasma, therefore reinforcing the potential on the development of autologous scaffolding architectures based on this protein concentrate. The elimination of immunogenic and disease transmission concerns due to its autologous origin are important advantages on the use of these materials.

There is an interest in developing GF-loaded scaffolds for TE strategies, aiming to boost the regeneration capacity of these materials. Nevertheless, several conventional methodologies for scaffold production and GF immobilization require the use of organic solvents and/or high processing temperatures, which hampers the preparation of scaffolds loaded with active GFs. In order to overcome these limitations, carbon dioxide (CO₂) has been used as an agent to form 3D scaffolds.

Our methodology enabled to produce a stable PL scaffold without the addition of an extra polymeric matrix, overcoming the traditional lack of stability and quick shrinkage of 3D hydrogels and scaffolds based on PL. The PL scaffolds crosslinked with genipin were characterized in terms of their morphological, mechanical, chemical, and biological performance by different techniques. Furthermore, the dispersion

of bioactive particles of BG within the 3D architecture enhanced the mechanical properties of the scaffold and promoted the growth of a calcium phosphate layer on the surface, similar to HA present in the bone. Moreover, it enabled the automatic formation of a bilayered structure, composed by one BG-enriched region and one BG-poor side. This functionally graded scaffold is suitable for application in osteochondral tissue engineering, as it could be placed in contact with cartilage and subchondral bone tissue. Cellular studies with our proposed structures were also promising, demonstrating that PL scaffolds were suitable templates for cell adhesion, proliferation, and colonization of the 3D structure.

The development of PL-based bilayered scaffolds for osteochondral tissue engineering, with the dual role of acting as a structural template and GFs source for the interface regeneration, represents a major advance in the state of the art in this field.

Acknowledgements The research leading to these results has received funding from the project “Accelerating tissue engineering and personalized medicine discoveries by the integration of key enabling nanotechnologies, marine-derived biomaterials and stem cells,” supported by Norte Portugal Regional Operational Programme (NORTE 2020), under the PORTUGAL 2020 Partnership Agreement, through the European Regional Development Fund (ERDF).

References

1. Yang PJ, Temenoff JS (2009) Engineering orthopedic tissue interfaces. *Tissue Eng. Part B Rev.* 15:127–141
2. Ahmed TAE, Hincke MT (2010) Strategies for articular cartilage lesion repair and functional restoration. *Tissue Eng. Part B. Rev.* 16:305–329
3. Lefebvre V, Smits P (2005) Transcriptional control of chondrocyte fate and differentiation. *Birth Defects Res Part C Embryo Today Rev* 75:200–212
4. Malafaya PB, Silva GA, Reis RL (2007) Natural-origin polymers as carriers and scaffolds for biomolecules and cell delivery in tissue engineering applications. *Adv Drug Deliv Rev* 59:207–233
5. O’Shea TM, Miao X (2008) Bilayered scaffolds for osteochondral tissue engineering. *Tissue Eng. Part B. Rev.* 14:447–464
6. Chen J et al (2011) Simultaneous regeneration of articular cartilage and subchondral bone in vivo using MSCs induced by a spatially controlled gene delivery system in bilayered integrated scaffolds. *Biomaterials* 32:4793–4805
7. Mano JF, Reis RL (2007) Osteochondral defects: present situation and tissue engineering approaches. *J. Tissue Eng. Regen. Med.* 1:261–273
8. Chen FM, Zhang M, Wu ZF (2010) Toward delivery of multiple growth factors in tissue engineering. *Biomaterials* 31:6279–6308
9. Kon E, Mutini A, Arcangeli E, Delcogliano M, Filardo G, Nicoli Aldini N, Pressato D, Quarto R, Zaffagnini S, Marcacci M (2008) Novel nanostructured scaffold for osteochondral regeneration: pilot study in horses. *J. Tissue Eng. Regen. Med.* 2:408–417
10. Lu HH, Subramony SD, Boushell MK, Zhang X (2010) Tissue engineering strategies for the regeneration of orthopedic interfaces. *Ann. Biomed. Eng.* 38:2142–2154
11. Anitua E et al (2006) New insights into and novel applications for platelet-rich fibrin therapies. *Trends Biotechnol* 24:227–234
12. Haberhauer M et al (2008) Cartilage tissue engineering in plasma and whole blood scaffolds. *Adv. Mater.* 20:2061–2067

13. Santo VE et al (2012) Enhancement of osteogenic differentiation of human adipose derived stem cells by the controlled release of platelet lysates from hybrid scaffolds produced by supercritical fluid foaming. *J. Control. Release* 162:19–27
14. Duarte a RC, Mano JF, Reis RL (2009) Perspectives on: supercritical fluid technology for 3D tissue engineering scaffold applications. *J. Bioact. Compat. Polym.* 24:385–400
15. Duarte ARC et al (2013) Unleashing the potential of supercritical fluids for polymer processing in tissue engineering and regenerative medicine. *J. Supercrit. Fluids* 79:177–185
16. Santo VE, Duarte ARC, Gomes ME, Mano JF, Reis RL (2010) Hybrid 3D structure of poly(D,L-lactic acid) loaded with chitosan/chondroitin sulfate nanoparticles to be used as carriers for biomacromolecules in tissue engineering. *J Supercrit Fluids* 54:320–327
17. van de Witte P, Dijkstra PJJ, van den Berg JWA, Feijen J (1996) Phase separation processes in polymer solutions in relation to membrane formation. *J. Memb. Sci.* 117:1–31
18. Eckert CA, Knutson BL, Debenedetti PG (1996) Supercritical fluids as solvents for chemical and materials processing. *Nature* 383:313–318
19. Temtem M et al (2009) Supercritical CO₂ generating chitosan devices with controlled morphology. Potential application for drug delivery and mesenchymal stem cell culture. *J. Supercrit. Fluids* 48:269–277
20. Keeney M, Pandit A (2009) The osteochondral junction and its repair via bi-phasic tissue engineering scaffolds. *Tissue Eng. Part B. Rev.* 15:55–73
21. Gadjanski I, Vunjak-Novakovic G (2015) Challenges in engineering osteochondral tissue grafts with hierarchical structures. *Expert Opin. Biol. Ther.* 2598:1–17
22. Nukavarapu SP, Dorcenus DL (2012) Osteochondral tissue engineering: current strategies and challenges. *Biotechnol Adv.* <https://doi.org/10.1016/j.biotechadv.2012.11.004>
23. Canadas RF, Marques AP, Reis RL, Oliveira JM (2017) In: Oliveira JM, Reis RL (eds) *Regenerative strategies for the treatment of knee joint disabilities*. Springer International, Berlin, pp 213–233. https://doi.org/10.1007/978-3-319-44785-8_11
24. Yan LP et al (2015) Bilayered silk/silk-nanoCaP scaffolds for osteochondral tissue engineering: In vitro and in vivo assessment of biological performance. *Acta Biomater.* 12:227–241
25. Yan LP, Oliveira JM, Oliveira AL, Reis RL (2013) Silk fibroin/nano-CaP bilayered scaffolds for osteochondral tissue engineering. *Key Eng. Mater.* 587:245–248
26. Zaky SH, Ottonello A, Strada P, Cancedda R, Mastrogiacomo M (2008) Platelet lysate favours in vitro expansion of human bone marrow stromal cells for bone and cartilage engineering. *J. Tissue Eng. Regen. Med.* 2:472–481
27. Santo VE et al (2016) Engineering enriched microenvironments with gradients of platelet lysate in hydrogel fibers. *Biomacromolecules* 17:1985–1997
28. Babo PS et al (2016) Assessment of bone healing ability of calcium phosphate cements loaded with platelet lysate in rat calvarial defects. *J. Biomater. Appl.* 31:637–649
29. Yan L, Oliveira JM, Oliveira AL, Reis RL (2015) Current concepts and challenges in osteochondral tissue engineering and regenerative medicine. *ACS Biomater. Sci. Eng.* 1(4):150220124046001. <https://doi.org/10.1021/ab500038y>
30. Ribeiro V, Pina S, Oliveira JM, Reis RL (2017) In: Oliveira JM, Reis RL (eds) *Regenerative strategies for the treatment of knee joint disabilities*. Springer International, Berlin, pp 129–146. https://doi.org/10.1007/978-3-319-44785-8_7
31. Cengiz IF, Oliveira JM, Reis RL (2014) In: Magnenat-Thalmann N, Ratib O, Choi HF (eds) *3D multiscale physiological human*. Springer, London, pp 25–47. https://doi.org/10.1007/978-1-4471-6275-9_2
32. Wang C, Lau TT, Loh WL, Su K, Wang D (2011) Cytocompatibility study of a natural biomaterial crosslinker—Genipin with therapeutic model cells. *J Biomed Mater Res B Appl Biomater* 97:58–65. <https://doi.org/10.1002/jbm.b.31786>
33. Muzzarelli RAA (2009) Genipin-crosslinked chitosan hydrogels as biomedical and pharmaceutical aids. *Carbohydr. Polym.* 77:1–9

34. Butler MF, Ng Y, Pudney PDA (2003) Mechanism and kinetics of the crosslinking reaction between biopolymers containing primary amine groups and Genipin. *J Polym Sci Part A Polym Chem* 41:3941–3953
35. Mu C, Zhang K, Lin W, Li D (2012) Ring-opening polymerization of genipin and its long-range crosslinking effect on collagen hydrogel. *J Biomed Mater Res A* 101:385–393. <https://doi.org/10.1002/jbm.a.34338>
36. Chuang M, Johannsen M (2009) Characterization of pH in aqueous CO₂—systems. *Polym Degrad Stab* 97(6):839–848
37. Babo P et al (2014) Platelet lysate membranes as new autologous templates for tissue engineering applications. *Inflamm. Regen.* 34:033–044
38. Santo VE, Popa EG, Mano JF, Gomes ME, Reis RL (2015) Natural assembly of platelet lysate-loaded nanocarriers into enriched 3D hydrogels for cartilage regeneration. *Acta Biomater.* 19:56–65
39. Duarte ARC, Caridade SG, Mano JF, Reis RL (2009) Processing of novel bioactive polymeric matrixes for tissue engineering using supercritical fluid technology. *Mater. Sci. Eng. C* 29:2110–2115
40. Rezwani K, Chen QZ, Blaker JJ, Boccaccini AR (2006) Biodegradable and bioactive porous polymer/inorganic composite scaffolds for bone tissue engineering. *Biomaterials* 27:3413–3431
41. Rey C, Combes C (2016) Biom mineralization and biomaterials. pp 95–127. <https://doi.org/10.1016/B978-1-78242-338-6.00004-1>